ISSN 1063-7826, Semiconductors, 2020, Vol. 54, No. 9, pp. 1069–1074. © Pleiades Publishing, Ltd., 2020.
Russian Text © The Author(s), 2020, published in Fizika i Tekhnika Poluprovodnikov, 2020, Vol. 54, No. 9, pp. 878–883.

XXIV INTERNATIONAL SYMPOSIUM
"NANOPHYSICS AND NANOELECTRONICS",
NIZHNY NOVGOROD, MARCH 10–13, 2020

Investigation into Microwave Absorption in Semiconductors for Frequency-Multiplication Devices and Radiation-Output Control of Continuous and Pulsed Gyrotrons

K. V. Maremyanin[a], V. V. Parshin[b], E. A. Serov[b], V. V. Rumyantsev[a,*], K. E. Kudryavtsev[a], A. A. Dubinov[a], A. P. Fokin[b], S. S. Morosov[c], V. Ya. Aleshkin[a], M. Yu. Glyavin[b], G. G. Denisov[b], and S. V. Morozov[a]

[a] *Institute for Physics of Microstructures, Russian Academy of Sciences, Nizhny Novgorod, 603950 Russia*
[b] *Institute of Applied Physics, Russian Academy of Sciences, Nizhny Novgorod, 603950 Russia*
[c] *Lobachevsky State University of Nizhny Novgorod, Nizhny Novgorod, 603950 Russia*
**e-mail: rumyantsev@ipmras.ru*

Received April 15, 2020; revised April 21, 2020; accepted April 21, 2020

Abstract—The results of experimental investigation into the dielectric losses in GaAs, InP:Fe, and Si semiconductor crystals in the millimeter wavelength range (80–260 GHz) using the original precise method of measuring the reflectance and dielectric-loss tangent $\tan\delta$ based on open high-quality Fabry–Perot cavities are presented. It is shown that the losses in the frequency range from 100 to 260 GHz in ultrapure semiconductor single-crystal GaAs substrates are mainly determined by lattice absorption, while the main loss mechanism in single-crystal silicon is absorption by free carriers; herewith, $\tan\delta \approx (1–2) \times 10^{-4}$ even for a noticeable, at a level of 10^{12} cm^{-3}, free carrier concentration. In contrast with GaAs and Si, $\tan\delta$ in compensated InP:Fe crystals is almost independent of frequency in the range from 100 to 260 GHz, which is associated with the material conductivity and optimization of microwave semiconductor devices, in particular, frequency-multiplication devices and devices of the controlled emission output of continuous and pulsed gyrotrons.

Keywords: subterahertz range, GaAs, InP:Fe, Si, absorption, dielectric-loss tangent
DOI: 10.1134/S1063782620090195

1. INTRODUCTION

High-power sources of coherent radiation of the far infrared (FIR) and terahertz (THz) ranges are in practical demand to solve many problems of a fundamental and applied character such as the development of new spectroscopy methods for semiconductor structures and biological objects [1], control over chemical reactions [2], manipulation by electron states in quantum wells [3], etc. The complexity of the development of such sources of the FIR/THz range is associated with the fact that approaches to the construction of emitting devices developed for optical or microwave regions are poorly applicable in this case. At the same time, to develop high-power radiation sources in the mentioned ranges (and subsequent broad use at the laboratory level) we could rely on nonlinear transformation of the emission frequency of gyrotrons [4] providing generation in the subterahertz (sub-THz) and THz ranges with a high output power both in the pulsed and continuous modes [5–7]. The development of such an approach requires the solution of such engineering and technical problems as the development of optical keys for controlling the output of gyrotrons and frequency multipliers to extend the working frequency range. Both these problems can be potentially solved when applying semiconductor materials as controllable mirrors or nonlinear elements. We note that along with an increase in the frequency, the development of controllable semiconductor mirrors opens up the possibility of implementing active compressors making it possible to provide nanosecond emission pulses with a power level of hundreds of MW, which is of interest for problems of high-gradient particle acceleration [8]. The necessity of operation of such devices in a high-power gyrotron radiation beam determines the requirement of the weak absorption of microwave radiation by the used materials to avoid their overheating and, finally, mechanical destruction.

Investigation into dielectric losses in various semiconductor materials in the millimeter and THz ranges seems to be important for the development of a corresponding element base for high-power devices and

systems. Despite a notable number of works on this theme [9–17], available published data seem to be far from complete. In this work, we present the results of measurements of the absorption (tanδ) of a series of semiconductors, notably, GaAs, Si, and InP:Fe, in the sub-THz spectral region and discuss certain aspects of device applications of the mentioned materials in problems of frequency multiplication and controlling flows of high-power microwave radiation.

2. SAMPLES UNDER STUDY

Interest in high-purity GaAs and Si crystals is due to the possibility of constructing optically controlled semiconductor mirrors for microwave radiation on their base. The "switching on" of such a mirror can be performed due to "illumination" by high-power band-to-band radiation forming a reflecting mirror with "quasi-metallic" conductivity near the semiconductor surface due to a high concentration of nonequilibrium carriers, $\sim(10^{18}–10^{19}\ cm^{-3})$; a similar concept was presented at the megawatt power level in some works [18–20]. The Fresnel reflection from such a mirror in the "switched-off" state (without illumination) can be minimized due to the destructive interference of waves reflected from the front and back plate faces. The question of studying dielectric losses and minimizing the absorption of high-power sub-THz radiation in semiconductor plates forming such an "optical key" is critical here.

As for InP, this material is interesting due to a larger quadratic susceptibility of the crystal lattice ($\chi^{(2)} \approx 3.45 \times 10^{-8}$ cm/V; for comparison, for GaAs, $\chi^{(2)} \approx 5.7 \times 10^{-9}$ cm/V [21]). Thus, InP can be used in problems of multiplying the gyrotron-radiation frequency to form intense THz and sub-THz beams. In particular, it is shown in [22] that the efficiency of nonlinear transformation during generation of the second harmonic in InP:Fe crystals can reach 3%.

In this work, we studied plates of high-purity GaAs with a resistivity (R) no lower than 10 MΩ cm and Si plates with a resistivity at a level of units of kΩ cm. The samples of InP crystals were compensated by iron (InP:Fe) to decrease the background concentration of free charge carriers. The parameters of the studied samples are presented in Table 1.

3. PROCEDURE FOR MEASURING THE DIELECTRIC LOSSES

In this work, we used the method of measuring ultrasmall losses in dielectrics using high-quality open Fabry–Perot cavities [23–26]. The quantities measured for calculation of the refractive index and dielectric-loss tangent are resonant frequencies of the widths of the resonant curve of the empty and loaded cavity. Measurements were performed at resonance frequencies of the analyzed samples, at which the integer number of the half-waves is laid over the plate thickness. The sample arrangement in the cavity was selected so that the sample planes coincided with the maxima or minima of the standing-wave electric field in the cavity according to recommendations formulated in [27]. We note that this procedure for measuring the reflectance n and tanδ of plane-parallel plates does not require individual determination of the plate thickness.

The radiation source is a backward wave tube with a precision digital frequency self-controlling system based on frequency phase self-tuning over synthesizer harmonics with the reference-frequency quantum standard controlled by a computer. To record the shape of the cavity resonance curve, we used a rapid scanning system over the frequency f in the phase self-tuning mode with conservation of the radiation phase under switching. The measurement accuracy of the resonance-curve width at a characteristic resonance of ~200 kHz of measuring the resonant curve width after averaging ~500 double-sided scans reached 20 kHz, which corresponded to a measurement error of tanδ at a level of $\sim(10^{-7}–10^{-6})$. These values exceed the sensitivity of the spectrometers constructed according to other schemes by more than an order of magnitude [28] and is sufficient for studying all modern dielectrics.

4. RESULTS AND DISCUSSION

4.1. Measurement of the Magnitude of the Dielectric Losses in GaAs and Si

The results of measuring the magnitude of losses (dielectric-loss tangent tanδ) for the considered GaAs and Si samples are presented in Table 1. The value of tanδ increases with frequency (Fig. 1); herewith, the data that are obtained for various samples fit well one model curve corresponding to the quadratic dependence of the losses on frequency. A similar frequency dependence was predicted in [9] for lattice absorption by means of "differential" two-phonon processes, notably, photon absorption with the frequency ω is accompanied by phonon emission with the frequency ω_1 and phonon absorption with the frequency $\omega_2 = \omega_1 - \omega$. We note that in addition to the "quadratic" part of the losses, noticeable "support" is also seen in Fig. 1, which is characterized by a weaker frequency dependence. The presence of such a "background" can be attributed to the contribution of other differential two-phonon processes, for which the resonance frequency is far from the range under study. It is important that the measured magnitude of losses (tanδ) in the GaAs plates under study is independent of the concentration n of free carriers (for rather pure samples with $n < 10^8\ cm^{-3}$), and "lattice" absorption is indeed the main (and irremovable in principle) mechanism of losses in the GaAs samples under study.

Table 1. Parameters of the samples under study and results of measurement of the reflectance $\tilde{n}$ and the dielectric-loss tangent $\tan\delta$

Materials	Frequency f, THz	$\tilde{n}$	$\tan\delta$, 10^{-4}
Gallium arsenide (GaAs), sample 1, $R > 10^7$ Ω cm	82.54	3.588	2.7
	165.08	3.597	3
	247.62	3.589	3.8
Gallium arsenide (GaAs), sample 2, $R = (1.41–4.4) \times 10^8$ Ω cm	123	3.592	2.8
	148	3.592	2.9
	172	3.592	3.1
	197	3.592	3.3
Indium phosphide (InP:Fe), sample 1, $R > 10^7$ Ω cm	130.12	3.527	4.7
	195.17	3.539	4.6
	260.26	3.532	4.6
Indium phosphide (InP:Fe), sample 2	200.80168	3.534	4.5
	194.71756	3.534	4.6
	188.64189	3.534	4.5
	182.5599	3.534	4.6
	176.46374	3.533	4.6
	170.38461	3.535	4.7
	164.29418	3.534	4.7
	158.21386	3.534	4.7
	152.13162	3.533	4.85
	146.0445	3.534	4.85
	139.95624	3.534	4.8
	133.87197	3.534	4.8
	127.78492	3.534	4.8
	121.70348	3.534	4.75
	115.61746	3.535	4.8
	109.53387	3.534	4.75
Indium phosphide (InP:Fe), sample 3, $R > 5 \times 10^6$ Ω cm	85.82	3.525–3.528	4.8
	128.71	3.534–3.537	5
	171.63	3.530–3.533	4.8
	214.655	3.533	4.4
Indium phosphide (InP:Fe), sample 4	109.530	3.534	4.7
	200.800	3.534	4.7
Silicon (Si), $N \approx 6.5 \times 10^{11}$ cm^{-3}, n-type	135.9	3.415	1.7
	203.794	3.415	1.1
Silicon (Si), $N \approx 2.2 \times 10^{12}$ cm^{-3}, p-type	168.505	3.42	1.6
Silicon (Si), $N \approx 2.3 \times 10^{12}$ cm^{-3}, n-type	168.505	3.42	4.8

The results of studying the reflectance n and quantity $\tan\delta$ for several c-Si samples are also shown in Table 1 and in Fig. 2. It is seen that the magnitude of losses in silicon in the frequency range under consideration is noticeably smaller than in gallium arsenide. This is explained by the fact that the structure of the silicon crystal lattice facilitates suppression of the multiphonon "lattice" component of losses; in this case, the losses associated with the conductivity of free carriers give the main contribution to material absorption in the sub-THz range. Such an assumption is confirmed both by an inversely proportional dependence

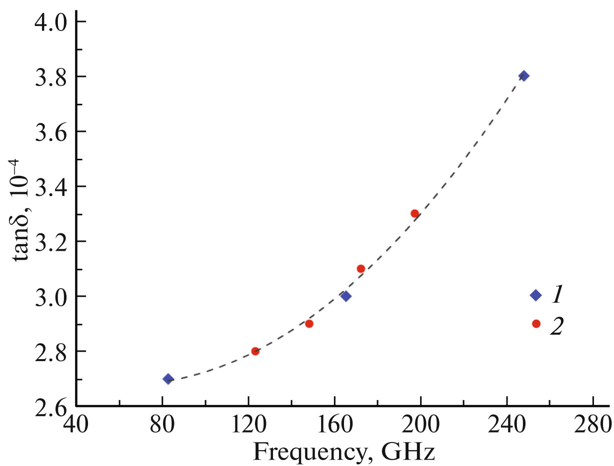

Fig. 1. Frequency dependences of the dielectric-loss tangent tanδ for two samples of GaAs semiconductor crystals.

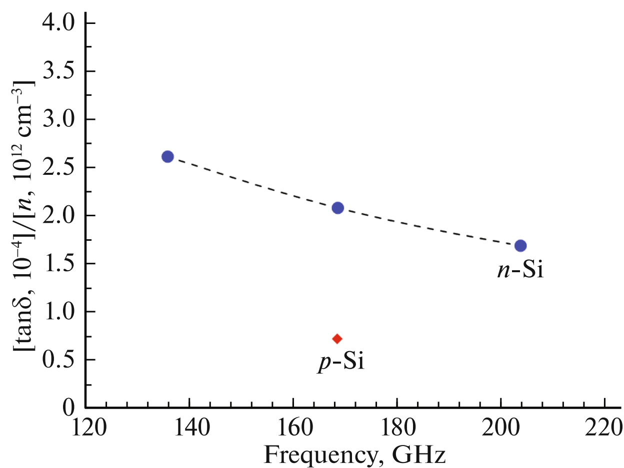

Fig. 2. Absorption (tanδ) for silicon plates of *n*-type and *p*-type conductivity. The data presented in the figure are normalized to the free carrier concentration in the samples under study (in units of 10^{12} cm^{-3}).

of tanδ on the test radiation frequency and by a proportional rise in losses in the samples with an increase in the free carrier concentration.

Despite the fact that the Si samples under study are characterized by a relatively high residual impurity concentration (~10^{12} cm^{-3}), the resulting magnitude of losses (tanδ) is noticeably smaller than in high-purity GaAs crystals. When compared with GaAs, a higher thermal conductivity and, in general, higher beam resistance are characteristic of silicon. In addition, the smaller absorptance at the band-to-band transition in the visible and near-IR spectral regions makes it possible to implement a more uniform reflecting layer with a high concentration of nonequilibrium carriers of the desired thickness (at a level of tens of μm) with the optical pumping of silicon plates. We note that the band-gap width both for GaAs and Si is extremely "convenient" for pumping by available and practical high-power solid or semiconductor lasers—for example, Nd:YAG. From this viewpoint, GaAs and Si are much more practical than diamond, although the latter is also characterized by a very low level of dielectric losses. A certain advantage of GaAs as the base for controlled semiconductor mirrors (when compared with Si) is the rather rapid "switching time" of such a mirror due to the short lifetime (~1 ns) of excess carriers in a direct-gap semiconductor, which potentially makes it possible to form nanosecond THz and sub-THz radiation pulses. As for silicon, to implement such a fast-operating optical key, it is necessary to substantially decrease the (nonradiative) nonequilibrium carrier lifetime, for example, due to doping by gold. It is known that the doping of silicon by gold will lead to recombination enhancement according to the Shockley–Read–Hall mechanism and will make it possible to retain a low level of losses in the sub-THz range [10, 17].

4.2. Measurement of the Dielectric Losses in InP:Fe

The results of measurement of the losses tanδ for the InP:Fe samples are presented in Table 1 and in Fig. 3. Previously, the authors of [14] investigated the dielectric losses in InP:Fe crystals in the region of noticeably larger frequencies; the observed features were attributed to lattice absorption, the magnitude of which was in general rather substantial and led to tanδ > 10^{-3} at frequencies f > 0.3 THz (herewith, the value of 10^{-3} corresponded to the measurement error). The application of a more sensitive measurement procedure in this work made it possible to accurately measure the magnitude of dielectric losses in the range of 100–260 GHz (Fig. 3). It is interesting that the magnitude of tanδ for the InP:Fe samples have no pronounced frequency dependence in the range of 100–260 GHz and in fact comprises a "plateau" in the limits of 10%.

We could have proposed the following hypothesis for explanation of the observed "plateau" of the magnitude of tanδ: the contribution of absorption by carriers increases in the range under consideration with a decrease in the radiation frequency, which compensates the drop in the magnitude of "lattice" (phonon) absorption in the lower frequency region. Indeed, the values of tanδ at frequencies of 250–260 GHz found in this work are lower by more than twofold when compared with those presented in [14] and, thus, correspond well to the long-wavelength shoulder of the absorption line associated with differential LO–TO phonon processes (between longitudinal and transverse optical phonons). At the same time, at a fixed conductivity $\sigma = en\mu$ (which is no larger than 10^{-6} $(\Omega\ cm)^{-1}$ for the samples under study), where n and μ are the electron concentration and mobility in InP,

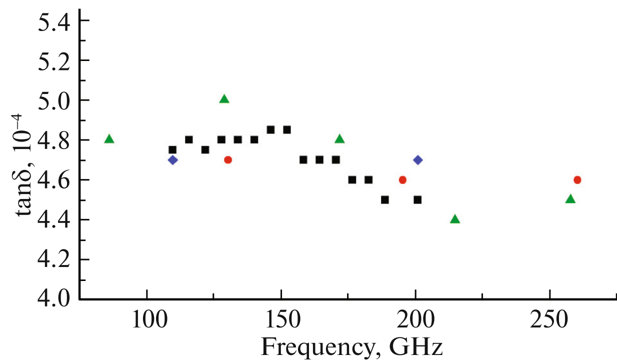

Fig. 3. Frequency dependences of the dielectric-loss tangent tanδ for samples of an InP:Fe compensated crystal.

respectively, estimation of the absorption by free carriers from the relationship

$$\tan\delta = \frac{\mathrm{Im}\,\varepsilon}{\mathrm{Re}\,\varepsilon} \sim \frac{\gamma_p}{\omega}\frac{\omega_p^2}{\omega^2+\gamma_p^2},$$

where $\gamma_p = e/(m^*\mu)$ and $\omega_p = 4\pi ne^2/(m^*\varepsilon_\infty)$, e is the elementary charge, $m^* = 0.08m_0$ is the effective mass, and $\varepsilon_\infty \approx 9.5$ is the high-frequency permittivity of InP, gives the magnitude of losses not exceeding $\tan\delta \sim 10^{-5}$. According to such estimation, absorption by free carriers is too weak and can determine only a small spread in the measured values of tanδ for various samples. As an alternative, it is possible to propose losses at localized carriers, which appear due to the sample conductivity in accordance with the hopping mechanism. Such a possibility is mentioned in [14] and was observed in [29], while the sublinear character of the frequency dependence of the hopping conductivity ($\sigma \propto \omega^\nu$, $\nu \le 1$ [30], $\nu \approx 0.7$–0.8 in [14]) makes it possible to explain the observed weak increase in losses with frequency; $\tan\delta \propto \omega^{(0.7-0.8)}/\omega$.

In general, the low losses and almost zero dispersion of the reflectance of InP:Fe in the studied spectral range allow us to count on a coherence length of ~(5–10) cm with frequency multiplication. In this case, the efficiency of nonlinear transformation can reach several percent with sufficiently moderate values of the radiation intensity (~50 kW/cm^2) at the fundamental frequency.

5. CONCLUSIONS

We measured the dielectric losses in GaAs, InP:Fe, and Si semiconductor crystals in the frequency range 100–260 GHz. It is shown that the main magnitude of losses in high-purity GaAs crystals is determined by lattice absorption according to the "differential" two-phonon mechanism. Phonon absorption in high-purity silicon is substantially suppressed, and the main mechanism of losses is absorption at free carriers according to the Drude mechanism, while the total magnitude of losses can be very small: $\tan\delta \approx (1$–$2) \times 10^{-4}$ even at a free carrier concentration of ~10^{12} cm^{-3}.

The measured values of the losses for InP:Fe crystals noticeably exceed the estimated values both for lattice absorption and for absorption by free carriers. We assumed that a noticeable contribution to the absorption of the microwave radiation in InP:Fe crystals can be associated with conduction according to the hopping mechanism. Our data can be useful for designing and optimizing microwave and terahertz semiconductor devices based on GaAs, InP:Fe, and Si.

FUNDING

This study was supported by the Russian Scientific Foundation, project no. 18-79-10112. The statement of the problem on using semiconductor mirrors in the compression circuit of pulses of megawatt gyrotrons for the high-gradient acceleration of particles and evaluation of the main parameters of semiconductors required to solve this problem are formulated in the Russian Science Foundation project no. 19-79-30071.

CONFLICT OF INTEREST

The authors declare that they have no conflict of interest.

REFERENCES

1. S. W. Smye, J. M. Chamberlain, A. J. Fitzgerald, and E. Berry, Phys. Med. Biol. **46**, R101 (2001).
2. N. Dudovich, D. Oron, and Y. Silberberg, Nature (London, U.K.) **418** (6897), 512 (2002).
3. B. E. Cole, J. B. Williams, B. T. King, M. S. Sherwin, and C. R. Stanley, Nature (London, U.K.) **410** (6824), 60 (2001).
4. A. V. Gaponov, M. I. Petelin, and V. K. Yulpatov, Radiophys. Quant. Electron. **10**, 794 (1971).
5. M. Thumm, J. Infrared, Millimeter, Terahertz Waves **41**, 1 (2020).
6. M. Y. Glyavin, G. G. Denisov, V. E. Zapevalov, M. A. Koshelev, M. Y. Tretyakov, and A. I. Tsvetkov, Phys. Usp. **59**, 595 (2016).
7. T. Idehara, S. P. Sabchevski, M. Glyavin, and S. Mitsudo, Appl. Sci. **10**, 980 (2020).
8. E. A. Nanni, W. R. Huang, K.-H. Hong, K. Ravi, A. Fallahi, G. Moriena, R. J. Dwayne Miller, and F. X. Kärtner, Nat. Commun. **6**, 8486 (2015).
9. B. M. Garin, in *Proceedings of the ICMWFST'96, 4th International Conference on Millimeter Wave and Far Infrared Science and Technology* (Beijing, China, 1996), p. 311.
10. B. A. Andreev, T. V. Kotereva, V. V. Parshin, V. B. Shmagin, and R. Heidinger, Inorg. Mater. **33**, 1100 (1997).
11. J. A. Hejase, P. R. Paladhi, and P. P. Chahal, IEEE Trans. Compon. Packaging, Manuf. Technol. **1**, 1685 (2011).

12. J. Krupka, J. Breeze, A. Centeno, N. Alford, T. Claussen, and L. Jensen, IEEE Trans. Microwave Theory Tech. **54**, 3995 (2006).
13. J. Krupka, J. G. Hartnett, and M. Piersa, Appl. Phys. Lett. **98**, 112112 (2011).
14. L. N. Alyabyeva, E. S. Zhukova, M. A. Belkin, and B. P. Gorshunov, Sci. Rep. **7**, 7360 (2017).
15. B. M. Garin, V. V. Parshin, S. E. Myasnikova, and V. G. Ralchenko, Diamond Relat. Mater. **12**, 1755 (2003).
16. R. Golovashchenko, V. Derkach, and S. Tarapov, Radiofiz. Elektron. **20** (4), 31 (2015).
17. J. Molla, R. Vila, R. Heidinger, and A. Ibarra, J. Nucl. Mater. **258–263**, 1884 (1998).
18. M. Kulygin and G. Denisov, J. Infrared, Millimeter, Terahertz Waves **33**, 638 (2012).
19. J. F. Picard, S. C. Schaub, G. Rosenzweig, J. C. Stephens, M. A. Shapiro, and R. J. Temkin, Appl. Phys. Lett. **114**, 164102 (2019).
20. A. A. Vikharev, G. G. Denisov, V. V. Kocharovsky, S. V. Kuzikov, V. V. Parshin, N. Y. Peskov, A. N. Stepanov, D. I. Sobolev, and M. Y. Shmelev, Radiophys. Quant. Electron. **50**, 786 (2007).
21. O. Madelung, *Semiconductors: Data Handbook* (Springer, New York, 2003).
22. V. V. Rumyantsev, K. V. Maremyanin, A. P. Fokin, A. A. Dubinov, V. V. Utochkin, M. Y. Glyavin, N. N. Mikhailov, S. A. Dvoretskii, S. V. Morozov, and V. I. Gavrilenko, Semiconductors **53**, 1217 (2019).
23. Y. A. Dryagin and V. V. Parshin, Int. J. Infrared Millimeter Waves **13**, 1023 (1992).
24. A. F. Krupnov, M. Y. Tretyakov, V. V. Parshin, V. N. Shanin, and M. I. Kirillov, Int. J. Infrared Millimeter Waves **20**, 1731 (1999).
25. V. V. Parshin, M. Y. Tretyakov, M. A. Koshelev, and E. A. Serov, Radiophys. Quantum Electron. **52**, 525 (2010).
26. V. N. Shanin, V. V. Dorovskikh, M. Y. Tretyakov, V. V. Parshin, and A. P. Shkaev, Instrum. Exp. Tech. **46**, 798 (2003).
27. E. V. Koposova, S. E. Myasnikova, V. V. Parshin, and S. N. Vlasov, Diamond Relat. Mater. **11**, 1485 (2002).
28. A. F. Krupnov, M. Y. Tretyakov, V. V. Parshin, V. N. Shanin, and S. E. Myasnikova, J. Mol. Spectrosc. **202**, 107 (2000).
29. N. F. Mott and E. A. Davis, *Electronic Processes in Noncrystalline Solids* (Oxford Univ. Press, London, 1971).
30. K. Khirouni, H. Maaref, J. C. Bourgoin, and J. C. Garcia, Mater. Sci. Eng. B **22**, 86 (1993).

Translated by N. Korovin